Excited State Energy Transfer Pathways in Photosynthetic Reaction Centers. 1. Structural Symmetry Effects

Robert J. Stanley, Brett King, and Steven G. Boxer*

Department of Chemistry, Stanford University, Stanford, California 94305-5080

Received: May 22, 1996[⊗]

Ultrafast excited state energy transfer to the primary electron donor or special pair in photosynthetic reaction centers has been measured following excitation of the lowest electronic state of the other chromophores. This was achieved by observing the rise time and induced anisotropy in the spontaneous fluorescence from the special pair using fluorescence up-conversion at 85 K. Very fast energy transfer is observed when exciting either of the bacteriochlorophyll monomers. Energy transfer from the bacteriopheophytins, which are considerably further from the special pair than the bacteriochlorophyll monomers, is about 50% slower. The rate, distance, and temperature dependence of energy transfer in both cases are very different from what is predicted by conventional Förster dipole−dipole theory. By working at low temperature and with the reaction center mutant (M)L214H (the beta mutant), which assembles with a bacteriochlorophyll monomer in place of a bacteriopheophytin in the H_L binding site (the location of the primary electron acceptor), it is possible to selectively initiate the energy transfer process on the functional and nonfunctional sides of the reaction center. The observed rates of energy transfer to the special pair are found to be similar. Thus *energy* transfer rates are comparable on the functional and nonfunctional sides, while *electron* transfer rates differ by at least 2 orders of magnitude. This suggests that the dominant source of functional asymmetry for electron transfer involves differences in the association of the functional-side chromophores with their environment (e.g. free and reorganization energy differences), rather than differences in electronic coupling.

The photosynthetic reaction center (RC) is designed to efficiently accept excitation energy from antenna complexes and rapidly transfer energy internally to the special pair primary electron donor, P. ^{1}P then transfers an electron within a few picoseconds to an electron acceptor, irreversibly trapping the excitation energy in a transient charge-separated species. A schematic diagram illustrating the chromophores that are relevant to both the energy and electron transfer processes in isolated RCs is shown in Figure 1A based on the X-ray structure,[1] and a putative excitation energy transfer scheme paralleling the structure is shown in Figure 1B. The chromophores labeled B_L and B_M are monomeric bacteriochlorophylls on the functional and nonfunctional sides, respectively, of the RC; the chromophores labeled H_L and H_M are monomeric bacteriopheophytins on the functional and nonfunctional sides, respectively. Functional is used here to denote the electron transfer process $^1P \rightarrow P^+H_L^-$, which is found to occur almost exclusively in normal RCs at all temperatures, despite the structural symmetry of the RC, which suggests that $^1P \rightarrow P^+H_M^-$ might be equally likely to occur. The physical origin of this functional asymmetry has been the subject of much investigation and speculation;[2−6] a recent paper provides some evidence for electron transfer down the nonfunctional side when the energetics are made relatively less favorable along the functional side.[7]

There are significant parallels between electron transfer and energy transfer when the latter is facilitated by the interpenetration of the donor and acceptor orbitals. These parallels have been considered extensively both theoretically[8,9] and experimentally in simple model systems.[10,11] Most treatments of electron transfer factor the rate into the product of an electronic coupling term, H_{DA}, and a Franck−Condon-weighted density of states term, which includes, at various levels of sophistication, the free energy change for the reaction and the reorganization energy associated with the response of the solvent (which may

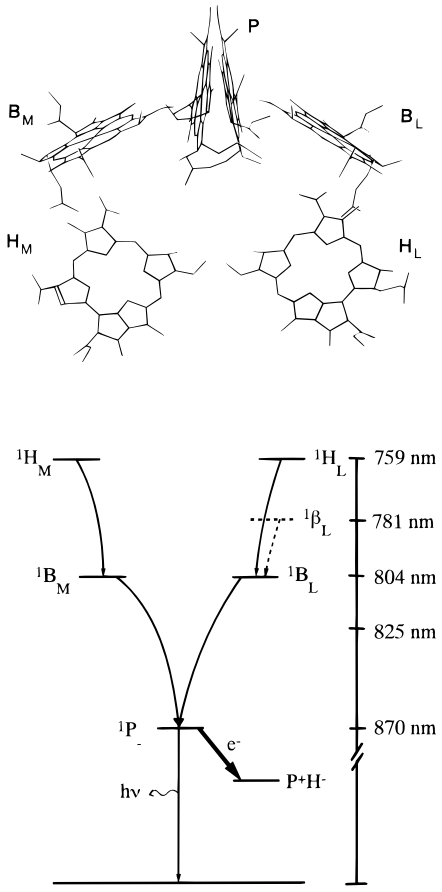

Figure 1. (A) Schematic diagram of the chromophores involved in the initial energy and electron transfer processes of *Rb. sphaeroides* photosynthetic reaction centers taken from the X-ray structure. (B) Schematic energy level diagram illustrating possible energy transfer pathways paralleling the structure in part A.

[⊗] Abstract published in *Advance ACS Abstracts,* July 15, 1996.

S0022-3654(96)01491-8 CCC: $12.00

be a protein) to the creation, destruction, or movement of charge and structural changes in the reactants themselves. The distance dependence of the electron transfer rate is primarily contained in the electronic coupling, which may fall off approximately exponentially with distance for a nonbonded system, although the falloff rate may be system specific; that is, it depends to a greater or lesser extent on the specific nature of the intervening medium.[12] Unlike electron transfer, where the electronic coupling, free and reorganization energies make substantial and largely independent contributions to the rate, which are often difficult to separate, electronic energy transfer (EET) by an exchange mechanism[10] depends on an electronic coupling term and spectral overlap, and the latter can be independently evaluated (in favorable cases) from spectroscopic data. The reorganization energy is expected to be small, as charged species are not changing. For singlet excited state energy transfer, EET theory was historically dominated by two paradigms depending on the distance between the donor and acceptor and whether the spectroscopic transition involved was allowed or forbidden. Dipole−dipole coupling (Förster theory)[13] has been used successfully when the point-dipole approximation is valid, typically at distances greater than 10 Å, where the details of the charge distribution on the donor and acceptors are relatively unimportant. In the range from ∼3 to 6 Å the Dexter exchange mechanism becomes important as the wave functions for the excited state donor and the ground state acceptor overlap significantly.[14] These two mechanisms are different limits of the same theory when the electromagnetic field is treated quantum mechanically (quantum electrodynamics).[15−17]

In the case of the RC, it is possible to study both singlet energy transfer and excited state electron transfer involving the same sets of chromophores. Breton et al.[18] measured excitation energy transfer lifetimes to P of <100 fs for excitation into the H and B absorption bands at room temperature in *Rhodopseudomonas viridis* by transient absorption and stimulated emission using 150 fs pulses (*vida infra*). Evidence from several laboratories[19,20] suggests that singlet energy transfer to P following excitation of the B chromophores, $^1BP \rightarrow B^1P$ (B_L and B_M excitation are not distinguished), is substantially faster than predicted by a Förster-type dipole−dipole energy transfer process; thus this process may occur by an exchange mechanism.[8] In the following we use fluorescence up-conversion to measure the kinetics of arrival of excitation energy on P following excitation of the H or B chromophores or of P directly in *Rhodobacter sphaeroides* RCs. In addition, we use an RC mutant that allows selective excitation of H_L and H_M (the beta mutant (M)L214H), where the chromophore occupying the H_L binding site is a bacteriochlorophyll instead of a bacteriopheophytin[21,22] to further probe the mechanism of ultrafast energy transfer and to determine whether structural symmetry breaking in the energy transfer process parallels that found for excited state electron transfer. In part II, we discuss the mechanism of energy transfer by measuring the transient population and decay kinetics of ^1B and by measuring energy transfer in mutants and modified RCs, where the properties of P are severely perturbed.[23]

Experimental Section

The low-temperature fluorescence up-conversion spectrometer has been described in detail previously.[24] Briefly, samples were excited using a mode-locked Ti:sapphire laser (Spectra Physics Tsunami) pumped by 6−10 W (all lines) from an argon-ion laser (Spectra Physics Model 2080). For these studies we have used an SF11 prism pair at the output of the Ti:sapphire laser to provide frequency compensation, reducing the pulse widths to ∼50 fs at 825 nm with a time−bandwidth product typically less than 0.38. The maximum pulse width used in these experiments was ∼81 fs for excitation at 760 nm. Samples were excited with <250 pJ of energy per pulse at 83 MHz. The fluorescence up-conversion spectrometer has been slightly modified in the following ways. We now use a 10 cm focal length, 90° off-axis parabola to focus the collimated fluorescence and gate beams into the BBO crystal; previously we had used a 18 cm focal length, 60° off-axis parabola. Separation of the sum frequency signal from the second-harmonic light generated from the gate beam is now achieved using a set of interference filters with a bandpass (fwhm) of 10 nm in addition to a 0.27 m monochromator. To obtain a valid zero of time, cross correlations were obtained from scatter of the excitation beam inside the sample by changing the wavelength of the monochromator and adjusting the phase-matching angle of the crystal, making no adjustment of the paraboloidal mirrors. Most decays were obtained with a delay line step size of 21 fs/point. Low temperature was achieved using a miniature Joule-Thompson refrigerator (MMR Technologies, Mountain View, CA) and a very thin sample geometry. Methane gas was used to cool the sample cell rapidly (<2 min) in air to 200 K before applying vacuum and switching to N_2 gas to produce a final working temperature of 85 K.

Anisotropy decays were obtained by rotating the polarization of the excitation beam using a zero-order quartz half-wave plate. A half-wave plate centered at 820 nm was inserted into the excitation arm of the spectrometer with the initial orientation set using a Glan-Thompson polarizer. The half-wave plate begins to depolarize the beam as the center wavelength moves a few tens of nanometers from the design wavelength of 820 nm (at 781 nm the depolarization is approximately 1%; a half-wave plate centered at 755 nm was used for measurements involving excitation at wavelengths shorter than 781 nm). The half-wave plate is rotated by a computer-controlled stepper motor so that the parallel and perpendicular components of the fluorescence decay can be taken sequentially with as little dead time as possible. Anisotropy values of 0.93−1.00 were obtained for excitation light scattered from the sample. A further check was obtained by exciting RCs directly into the P band at 847 nm, where we measured an anisotropy of 0.39−0.40 (the RCs used for this experiment were the *Rb. sphaeroides* mutant (M)-L214G, whose pigment content and absorption spectrum are identical to WT (see below), and the (M)L214H (beta) mutant, whose P band absorption is identical to WT). The time-dependent anisotropy decays, $r(t) = (I(t)_{\parallel} - I(t)_{\perp})/(2I(t)_{\perp} + I(t)_{\parallel})$, were constructed using the raw data with a correction factor for the 30° off-axis excitation geometry and the three interfaces that the parallel/perpendicular excitation beam traverses before exciting the sample. These three interfaces consist of air−CaF_2/CaF_2−vacuum/vacuum−borosilicate glass. We make no correction for the glass−glycerol/buffer interface, as the indices of refraction of these materials are too close to affect the calculated value of $r(t)$. The time-resolved anisotropies did not change with time (see below), so we report the anisotropies using the integrated areas under the parallel and perpendicular decays out to ∼3 ps, thereby obtaining better signal-to-noise for these values.

Wild-type (WT), (M)L214G, and (M)L214H (beta mutant) *Rb. sphaeroides* were grown semiaerobically. The (M)L214G mutant, produced in our laboratory by Joshua Goldsmith, introduces a cavity above H_L by replacing leucine 214 with a glycine. The beta mutant strain was generously provided by Professor C. Schenck, Colorado State University. By replacing Leu214 above H_L with a His residue, the Mg^{2+} ion is retained so that a bacteriochlorophyll *a* is found to occupy the H_L binding

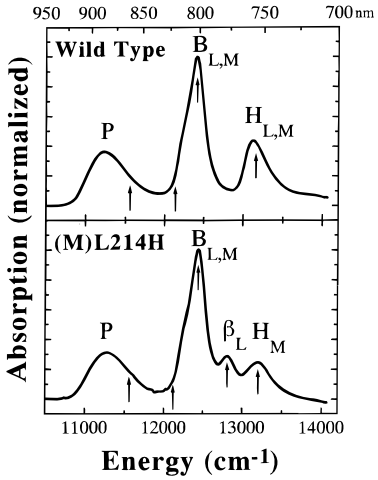

Figure 2. Electronic absorption spectra in the Q_y region at 77 K for *Rb. sphaeroides* (A) wild-type and (B) beta mutant (M)L214H in which a bacteriochlorophyll *a* labeled β_L replaces H_L.

site; this chromophore is denoted β_L.[21] By contrast, the (M)-L214G mutant has a normal pigment content and absorption spectrum whether or not the medium contains exogenous imidazole.[25,26] This strain was used as a surrogate for WT in several experiments. RCs from WT, (M)L214G, and the beta mutant were isolated and quinone-depleted by the method of Okamura et al.[27] These RCs all contain carotenoid, which is important for experiments using relatively high repetition rate excitation. All samples were dissolved in 1/1 (v/v) glycerol/buffer (10 mM Tris, pH 8.0) solution. The RCs were concentrated in order to achieve a sufficient OD in the 25−70 μm pathlength, typically 0.1−0.5. The absorption spectra in the Q_y region of WT and beta mutant RCs at 77 K are compared in Figure 2 with relevant absorption features and excitation wavelengths highlighted.

Data Analysis

Our goal is to extract information on the arrival time of excitation to P probed by the rise in the fluorescence from ^{1}P following excitation of the other chromophores in the RC or P itself. Even with excellent signal-to-noise data this is a nontrivial task, as the rise time of the fluorescence is not much longer than the instrument response function, which is itself dependent on the excitation wavelength. Furthermore, ^{1}P begins to decay on a time scale less than 1 order of magnitude longer than its rise due to electron transfer, and this decay is poorly described by a single-exponential function.[28,29] Finally, for some excitation wavelengths, oscillations are observed on the decay due to vibrational coherence following impulsive excitation.[24] Thus, even assuming, as we do, that each of the rise and decay processes can be modeled by using conventional rate constants, there is no entirely satisfactory approach to analyze the data. Given this dilemma, we have compared several different approaches.

In general, spontaneous fluorescence signals were fit to a sum of exponential functions. In the case where excitation energy transfer can be resolved, two or three exponentials were used with one having a negative amplitude to account for the energy transfer component. Because our goal is to obtain accurate rise times in the fluorescence (85−300 fs, *vide infra*), we did not usually measure a complete decay to base line, rather the decays were measured out to several picoseconds (more than five 1/e times for the rise time). A long time base scan (30−50 ps in extent) was performed to provide a check that the truncation of data sets (3−5 ps typically) did not introduce spurious values for the fast rise in the emission. Depending on the ^{1}P decay time, the second and/or third exponential components would vary considerably in the fitting procedure; however, the rise time of the negative amplitude component was usually stable whether the time window measured covered 3 or 30 ps, and this rise time is the focus of this paper.

The data were analyzed by three methods: a convolute-and-compare (C&C) fit to a multiexponential model function, a simultaneous convolute-and-compare fitting of comparable data sets to a multiexponential model function, and a linear prediction singular value decomposition procedure (LPSVD). We have previously analyzed fluorescence decays by the first method.[24] Since multiple data sets were taken for each excitation wavelength, we implemented the simultaneous fitting procedure as a check; generally the rise times of the fluorescence were very similar whether analyzed individually or simultaneously.

LPSVD is widely used for fitting data with oscillatory components,[30] but it is generally useful because it offers an objective measure of the minimum number of decay components that best describe the data set. Furthermore, this method reveals whether a negative amplitude component is present without the *a priori* assumption of its existence. The routine returns a table of lifetimes, amplitudes, frequencies, and phase factors corresponding to the model: $S(t) = \sum A_i e^{t/\tau_i} \cos(\omega_i t + \phi_i)$. If there is a feature that grows in with a rise time τ (e.g. excitation energy transfer), it appears as a negative amplitude component with zero frequency and a phase factor of 0°. A significant drawback of LPSVD arises for data resulting from a delta-function-like excitation event, as the sharp rise due to the excitation event is returned as a large number of large amplitude oscillatory components, which can effectively obscure the nonoscillatory rise and decay components.[31] Thus LPSVD is useful only after a specified amount of time has elasped between the excitation event (in this case the measured $t = 0$ obtained by fitting the cross correlation function to a Gaussian) and the beginning of the data analysis window.

Wise et al.[32] have addressed this problem by simulating pump-probe data and analyzing it using LPSVD. They found that fast decay components, on the order of the instrument response function fwhm, can be reliably returned from LPSVD even if the data set is analyzed after a time corresponding to one fwhm of the Gaussian cross correlation function of the simulated instrument response function. The S/N requirements for accurate rate constant retrieval for three-exponential functions is 60 dB (1000/1 S/N). They also showed that as the signal-to-noise of the data set worsens, there is a rapid deterioration of the accuracy of the values returned by the algorithm. We have implemented the algorithm according to the procedures outlined in Barkuijsen et al.,[33] and then, following Wise et al.,[32] using Poisson noise statistics we find that accurate fit parameters can be obtained for simulated data with twice the Poisson-distributed noise if the analysis begins after one sigma of the Gaussian cross correlation function used to generate the simulated data set. The error obtained when the simulated noise is twice the Poisson limit is ±5%. The noise in our experimental setup is not Poisson-distributed ($\sqrt{\text{counts}}$) because of factors such as mechanical vibration and digitization error of the delay line position; however, the simulated data sets serve to put limits on what one can expect from this type of analysis. In practice, the LPSVD values show a systematic trend toward longer lifetimes than C&C, which we interpret as an artifact of the convolution of the instrument response function (IRF) with the rise of the fluorescence. This is especially apparent when the H bands are excited at 760 nm because the IRF was typically greater than 120 fs and the rise time of the fluorescence signal

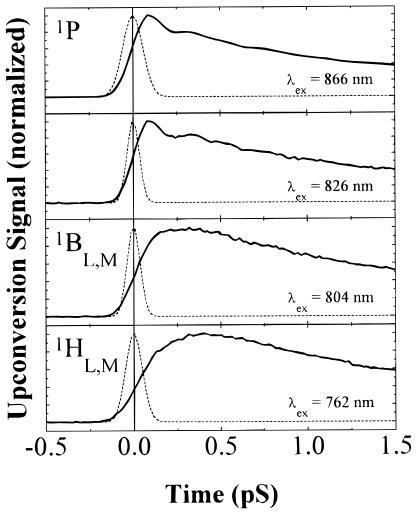

Figure 3. Spontaneous fluorescence from ^{1}P measured at 940 nm for wild-type RCs at 85 K following excitation (*cf.* Figure 2A) at (A) 866 nm (direct excitation of P); (B) 826 nm (excitation of the upper exciton band of P or a high-lying vibrational state); (C) 804 nm (excitation of B chromophores); and (D) 762 nm (excitation of H chromophores). The dotted lines show representative instrument response functions at the excitation wavelengths.

is about 300 fs (*vide infra*). Because of the superior ability to handle the deconvolution of the IRF, we use the C&C values for the decays; however the analysis of the oscillations on the decay is facilitated by using the LPSVD method.

Results

Excitation Energy Transfer in Wild-Type RCs. The rise and initial decay of the fluorescence from ^{1}P measured at 940 nm in WT RCs at 85 K following direct excitation of P at 866 nm, excitation at 826 nm (in the region of the upper exciton band of ^{1}P or a high-lying vibrational state, see below), at 804 nm (both B chromophores), and at 762 nm (both H chromophores) are shown in Figure 3 (*cf.* the absorption spectrum in Figure 2A). The emission wavelength of 940 nm was chosen to ascertain whether vibrational coherence was maintained in the EET process, as this is where the maximum amplitude oscillations are observed (*cf.* Vos et al.[34]). The emission wavelength of 920 nm was chosen for anisotropy measurements, as this is near the peak of the emission and provided the best S/N. When P is excited directly at 866 nm, the rise of the fluorescence is limited by the instrument response function, and no negative amplitude components were necessary to fit the data. Furthermore, as reported previously,[24] impulsive excitation of P gives rise to oscillations in the spontaneous fluorescence, as originally observed by stimulated emission.[34,35] As shown in Figure 4A, the time-resolved fluorescence anisotropy measured following excitation at 847 nm is close to 0.40, indicating that the angle between the P absorption and emission transition dipole moments is less than 15°.

As the excitation wavelength is moved to 826 nm, the kinetics, whether analyzed by C&C or LPSVD, always requires a negative amplitude component, indicative of an energy transfer process to the emitting state. Figure 3B shows the rise and initial decay of fluorescence from ^{1}P at 940 nm following excitation at 826 nm using ~50 fs pulses. This excitation wavelength was chosen because the upper exciton band of P, often denoted ^{1}P$_+$, is thought to contribute to the absorption under the B bands (with a putative peak absorption at 815 nm and extending to somewhat lower energy; 826 nm corresponds to minimal direct excitation of B).[36−39] The measured rise time

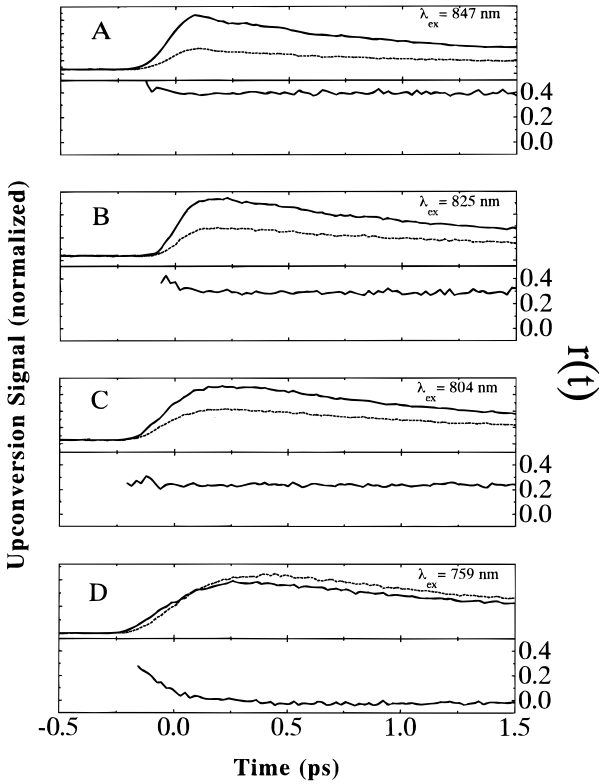

Figure 4. Fluorescence anisotropy decays for WT RCs at 85 K for different excitation wavelengths. All data were taken at an emission wavelength of 920 nm with a time resolution of 21 fs/point: (A) 847 nm (direct excitation of P); (B) 825 nm (excitation of the upper exciton band of ^{1}P or a high-lying vibrational state); (C) 804 nm (excitation of B chromophores); (D) 759 nm (excitation of H chromophores).

TABLE 1: Rise Times for Spontaneous Fluorescence from ^{1}P following Excitation at Various Wavelengths in Wild-Type and Beta Mutant Reaction Centers at 85 K

reaction center	λ_{ex} (nm)	τ_{LPSVD} (fs)	$\tau_{C\&C}$ (fs)	r
wild-type[a]	825	88 ± 25[a]	71 ± 24[a]	0.323 ± 0.005
	804	147 ± 30[b]	163 ± 54[b]	0.241 ± 0.003
	759	257 ± 33	260 ± 32	$-0.015^{+0.01-0.002}$
(M)L214H (beta)	825	111 ± 24	88 ± 17	0.275 ± 0.012
	804	170 ± 24	162 ± 25	0.231 ± 0.004
	781	206 ± 13	239 ± 35	0.082 ± 0.001
	759	254 ± 30	300 ± 11	0.016 ± 0.001

[a] This was also measured in the (M)L214G mutant, whose absorption properties are identical to WT, giving 129 ± 29 and 74 ± 12 fs for τ_{LPSVD} and $\tau_{C\&C}$, respectively. [b] This was also measured in the (M)L214G mutant, whose absorption properties are identical to WT, giving 154 ± 19 and 180 ± 19 fs for τ_{LPSVD} and $\tau_{C\&C}$, respectively.

of the fluorescence is 71 ± 24 fs, and oscillations are clearly evident on the decay (this was also observed for excitation at 818 nm, data not shown; see the discussion below). The values for the rise times in each case are summarized in Table 1. LPSVD was used to analyze the frequency components of the oscillations for excitation at 866 and 826 nm, and they were found to be comparable. The anisotropy decreases somewhat, giving a value of 0.323 ± 0.005 for excitation at 825 nm (Figure 4B), corresponding to an angle of 21 ± 1°.

Figure 3C shows the spontaneous fluorescence from ^{1}P following excitation directly into the B band at 804 nm using slightly longer pulses (62 fs). No oscillations are observed in the fluorescence decay within the signal-to-noise, and the rise time is best fit with a value of 163 ± 54 fs (Table 1). As shown in Figure 4C, the anisotropy is 0.241 ± 0.003 for excitation at this wavelength, corresponding to 32 ± 1° as the angle between

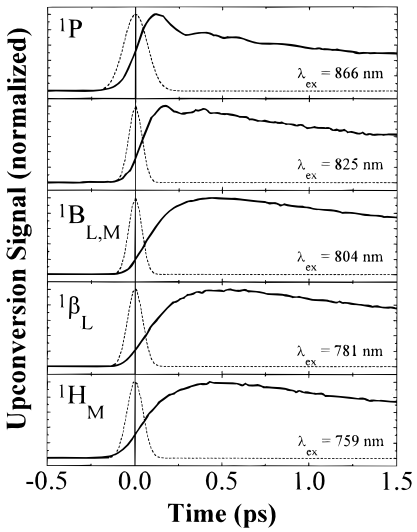

Figure 5. Spontaneous fluorescence from ^{1}P measured at 940 nm for beta mutant RCs at 85 K following excitation (*cf.* Figure 2B) at (A) 866 nm (direct excitation of P); (B) 825 nm (in the region of the upper exciton band of P or a high-lying vibrational state); (C) 804 nm (excitation of both B chromophores); (D) 781 nm (selective excitation of the β chromophore), and (E) 759 nm (selective excitation of the H_M chromophore).

the transition moment at 804 nm and the emission transition moment of ^{1}P. This is in good agreement with the steady state fluorescence anisotropy measurements in R-26 RCs by Ebrey and Clayton[40] and the linear dichroism measurements on *Rps. viridis* in stretched films by Breton[37] and is roughly as expected from the X-ray structure, making reasonable assumptions about the orientations of the transition dipole moments relative to the molecular axes.[41] The same value was also measured exciting at 818 nm, and the anisotropy was observed to have this value over a range of 30 ps (data not shown).

Figure 3D shows the rise and initial decay of ^{1}P fluorescence following selective excitation of the H bands at 762 nm (~84 fs pulse width). The rise time for the fluorescence is 260 ± 32 fs from the C&C fit (Table 1); no oscillations are observed on the decay. For excitation at this wavelength, the anisotropy is $-0.015^{+0.01}_{-0.002}$ ($56.2^{+0.3}_{-0.8}$°).

Excitation Energy Transfer in Beta Mutant RCs. The rise and initial decay of the fluorescence from ^{1}P measured at 940 nm in beta mutant RCs at 85 K following direct excitation of P at 866 nm, excitation at 825 nm (in the region of the upper exciton band of ^{1}P or a high-lying vibrational state, see below), at 804 nm (both B chromophores), at 781 nm (selective excitation of the β_L chromophore, *cf.* Figure 2B), and at 759 nm (selective excitation of the H_M chromophore) are shown in Figure 5. As seen in Figure 2B, the absorption of the bacteriochlorophyll labeled β_L in the H_L binding site of this mutant is sufficiently different from the bacteriopheophytin in the H_M binding site at 85 K that each chromophore can be selectively excited, thereby initiating the energy transfer process on spatially (and functionally) distinct sides of the RC.

The decay of ^{1}P due to electron transfer is slower in the beta mutant than for WT and, when excited directly into the P band, exhibits oscillations as shown earlier.[24] Excitation of the beta mutant RC at 825 nm with emission set at 940 nm yields the same rise time (within experimental error) as was measured for WT, as well as oscillations in the decay. Analysis of the frequencies using LPSVD shows very good agreement between the values obtained using 866 nm excitation and 825 nm excitation, as for WT. Anisotropy measurements for this excitation wavelength (at 920 nm emission, data not shown) give $r = 0.273 \pm 0.012$ (27.4 ± 1.4°). Excitation of B at 804 nm, with emission at 940 nm, gives a rise time of 162 ± 25 fs at 85 K, essentially identical to the value obtained for WT, with no evidence for oscillations on the decay. The measured anisotropy of this band is also in agreement with that obtained for WT ($r = 0.231 \pm 0.004$, giving 32.1 ± 0.05°, data not shown). Selective excitation of the β_L chromophore in the H_L binding site at 781 nm gives a rise time of 239 ± 35 fs. The anisotropy of this band is very nearly zero with $r = 0.082 \pm 0.001$ (46.7 ± 0.1°, data not shown). Selective excitation of the bacteriopheophytin in the H_M binding site at 759 nm gives a rise time of 300 ± 11 fs. The anisotropy of this H_M band is also close to zero, with a value of $r = 0.016 \pm 0.001$ (53.1 ± 0.1°, data not shown).

Discussion

Direct excitation of P. The spontaneous fluorescence decay from ^{1}P following direct excitation of the Q_y transition of P has been reported by several groups.[24,28,42] The data at room temperature are roughly comparable, and we have also presented results at 85 K, where oscillations are clearly seen.[24] We observe that the rise is within the instrument function, consistent with the simple picture that the emitting and absorbing states are the same. Du et al. also reported room temperature energy transfer lifetimes of ~200 fs for R-26 quinone-depleted RCs with excitation at 608 nm.[28] While the 608 nm region of the RC absorption spectrum may be the result of several overlapping transition, the authors attribute the 200 fs lifetime to internal conversion of $^1P(Q_x) \rightarrow {}^1P(Q_y)$.

As the excitation pulse is tuned to higher energy, but not yet into the strong B-band absorptions around 800 nm, we are able to resolve a rise in the fluorescence measured at 920 or 940 nm. It is generally believed that the upper exciton band of the dimeric special pair, $^1P_+$, absorbs in this region, although the exact position, intensity, and temperature dependence of the upper exciton band are far from settled in the literature. In the simplest model, the transition moments for the upper and lower exciton components are orthogonal; thus one expects that the anisotropy induced in the lower exciton band upon excitation of the upper exciton band would be negative. The observed anisotropy, although smaller than when exciting the major P band directly at 847 nm, is never negative or even less than +0.3 in WT when exciting in this region. Similar results were obtained in steady state fluorescence excitation measurements published many years ago.[40] There are several plausible explanations for the somewhat reduced anisotropy associated with 825 nm excitation. The oscillator strength could be dominated by higher vibrational levels of the strongly allowed lower exciton component. Vibronic coupling would likely lead to a smaller projection of the absorbing and emitting transition moments, as is observed for chlorophyll *a*.[43] A second possibility is that there is some excitation of B at this wavelength. Because the rise time for direct excitation of the major B band at 804 nm is considerably longer than what is observed with 825 nm excitation, this seems unlikely, although it is possible that the energy transfer rate for excitation on the red edge of the B band is different from the center, as discussed in detail elsewhere.[23] Oscillations are observed on the decay, and we do not observe these oscillations when B is excited directly (see below).

Energy Transfer from ^{1}B to P. It is evident from the data for WT and the beta mutant that there is a delay between the excitation of B at around 800 nm and the appearance of emission from ^{1}P. Furthermore, within our signal-to-noise, there is no evidence for oscillations in the decay of ^{1}P. Jia et al. claim to

observe oscillations in the decay of ^{1}B following excitation at 800 nm of R-26 RCs at room temperature with 27 fs pulses.[20] Irrespective of this subtle issue, the major result confirms earlier data[19] demonstrating extremely rapid energy transfer from ^{1}B to P.

There are further interesting similarities and differences with the data of Jia et al. These authors obtained two decay times for the bleach of ^{1}B, a 116 ± 35 fs component with 60% of the amplitude and a 270^{+90}_{-40} fs component with 40% amplitude. By contrast, we do not observe a second slower component in the rise of the fluorescence from ^{1}P following excitation of B. A plausible explanation for the difference is that the very short 27 fs excitation pulses centered at 802 nm used by Jia et al. have a spectral half-width (given a time−bandwidth product of 0.35) extending to 788 nm. At room temperature the H absorption band contributes to the absorption at this wavelength. The slower component reported by Jia et al. is quite similar to what we observe with selective excitation of H (Table 1). Thus, a reasonable explanation of the slower component is that it corresponds to a fraction of H excitation (the slower component observed by Jia et al. corresponds closely to what we observe following selective excitation of H), rather than a more complex process involving ^{1}B itself, which we do not observe when B is selectively excited. Earlier transient absorption studies on *Rps. viridis* RCs at room temperature[18] with 150 fs pulses reported EET lifetimes of <100 fs for $^1\text{B} \rightarrow \text{P}$. In these studies it was proposed that a small fraction (10%) of the RCs decayed without EET to P with a lifetime of ~500 fs. We do not observe such a component.

While this work was in preparation, Haran et al.[44] and Wynne et al.[45] reported the anisotropy of the ^{1}B to P EET process measured by stimulated emission with $\lambda_{ex} = 810$ nm (pulse width ~60 fs) and $\lambda_{probe} = 950$ nm in dithiothreotol-treated *Rb. sphaeroides* R-26 RCs at room temperature. These authors obtained a value of $r = 0.11 \pm 0.01$, substantially lower than the value we have found for either $\lambda_{ex} = 802$ nm ($r = 0.241$) or $\lambda_{ex} = 825$ nm ($r = 0.323$) in both WT and beta mutant RCs or as was found in early steady state fluorescence measurements.[40] Assuming that the degraded anisotropy reported by Haran et al. and Wynne et al. is not due to experimental error, it is possible that the transient absorption and associated anisotropy probed at short times around 950 nm is not assignable solely to stimulated emission of ^{1}P but also includes contributions from states that have a substantially lower anisotropy. A second possibility is that the relatively higher excitation pump power used in the transient absorption measurements produces excitations that are not sampled with the substantially lower power pulses used in our spontaneous fluorescence measurements. Although spontaneous fluorescence is limited to providing information on the excited state kinetics of the emitting species, it does have the advantage, especially important for anisotropy measurements,[46] of avoiding overlapping bleach and absorption features. We conclude that the anisotropies reported by Haran et al. using transient absorption are likely considerably lower than the true value. Haran et al. interpret their observed low value of r compared with that estimated from the X-ray structure[47,48] in terms of a model in which there is strong mixing between the excited states of B and P.[49] Our observed value of r is consistent both with the value obtained by more conventional measurements[36,37,40] and that estimated from the X-ray structure using a localized picture; thus this basis for the model of mixed levels proposed by Haran et al. is not supported by our results.

As discussed in the introduction, simple estimates based on Förster dipole−dipole theory using the interchromophore distances estimated from the X-ray structure and optimal (parallel) geometries for the transition dipole moments suggest that the observed energy transfer rate is orders of magnitude too fast to be occurring by this mechanism alone.[8] Haran et al.[44] have re-evaluated this question and suggest that Förster energy transfer from ^{1}B to P is possible given that the P band, centered at 860 nm at room temperature, is broad, leading to appreciable spectral overlap between the hypothetical ^{1}B fluorescence (as no ^{1}B emission is observed, the actual Stokes shift in the RC is not known) and P band. They predict EET lifetimes at room temperature of 158 and 130 fs for $^1\text{B}_\text{L}$ and $^1\text{B}_\text{M}$, respectively, to P, comparable to the average value we measure. This apparent agreement is misleading, however, as we and others[18,20] have measured a similar EET rate for ^{1}B to P at 85 K. The P absorption band shifts substantially to lower energy and narrows by nearly a factor of 2 as the temperature is lowered from room temperature to cryogenic temperatures (see Figure 2; the absorption of B narrows, but does not shift appreciably). As a result, the spectral overlap between hypothetical ^{1}B emission and P absorption is at least 10-fold less at low temperature than room temperature; thus energy transfer, if it were occurring by the Förster dipole−dipole mechanism at low temperature, would be much slower than at room temperature, contrary to what we and others[18,20] observe. We have also measured the rise time in the fluorescence of ^{1}P following B excitation at 802 nm as a function of temperature from 82 to 200 K (data not shown). The temperature dependence is weak over this range (changing from 163 ± 54 fs^{-1} to 121 ± 25 fs^{-1}, respectively) despite the large shift of the absorption of P to lower energy. Finally, as shown elsewhere,[23] the energy transfer rate is not greatly affected when the absorption of P is substantially changed. Taken together these results suggests that the Förster dipole−dipole mechanism is likely not playing a significant role at *any* temperature. Given these results and the close physical proximity of B and P, we suggest, as others have before,[8] that direct orbital overlap dominates energy transfer between ^{1}B and P. As discussed below, we also have evidence that the rates of energy transfer from $^1\text{B}_\text{L}$ and $^1\text{B}_\text{M}$ to P are comparable.

Energy Transfer from ^{1}H to P. Energy transfer from ^{1}H to P can be accurately time-resolved despite our somewhat poorer IRF at 760 nm. The rate is slower than from ^{1}B by about 50%. This is remarkable as the distance between H and P is substantially greater than between B and P. This much greater distance, along with the negligible spectral overlap between H and P, makes the Förster mechanism for direct energy transfer between ^{1}H and P impossible. A more reasonable model is that energy transfer occurs sequentially, first from ^{1}H to B and then from ^{1}B to P.[50] Fixing the ^{1}B to P rate at 160 fs, as observed with direct excitation of B, we can model the excited state dynamics to obtain an estimate for the ^{1}H to B step, assuming a sequential mechanism. If ^{1}H to B is also about 160 fs, the calculated rise in ^{1}P fluorescence is predicted to be about 250 fs, close to the observed value. If the ^{1}H to B step is much slower than this, the calculated rise in ^{1}P fluorescence is slower than observed. It is plausible that the ^{1}H to B step occurs by the Förster dipole−dipole mechanism. The spectral overlap is quite reasonable (see, for example, Figure 2), and the absorption in this region does not change appreciably with temperature. A clear prediction of this sequential model is that a substantial population of ^{1}B should be present on the time scale of about 100 fs when H is excited selectively. This is discussed further elsewhere.[23]

Energy Transfer in WT vs the Beta Mutant and Implications for Asymmetric Electron Transfer. The beta mutant exhibits much the same EET kinetics and anisotropy charac-

teristics as those obtained for WT RCs for excitation at 825 and 804 nm (see Table 1). Selective excitation at 781 nm into the β_L chromophore leads to a slightly faster rate for EET (239 $\pm$ 35 fs^{-1}) than excitation into the H_M chromophore (300 $\pm$ 11 fs^{-1}). If $^1\beta_L \rightarrow P$ or $^1H_M \rightarrow P$ energy transfer is modeled as a sequential two-step process, i.e., $^1\beta_L \rightarrow B_L \rightarrow P$ or $^1H_M \rightarrow B_M \rightarrow P$, and using the directly measured $^1B \rightarrow P$ rate of about 160 fs^{-1} (note: the individual $^1B_L \rightarrow P$ and $^1B_M \rightarrow P$ processes are not distinguished in this direct measurement), then the initial $^1\beta_L \rightarrow B_L$ or $^1H_M \rightarrow B_M$ steps have comparable rates (the latter somewhat slower). Because the overall rates of energy transfer to P along the L and M branches are comparable, the implication, assuming a two-step sequential mechanism, is that the second step along each branch, $^1B_L \rightarrow P$ or $^1B_M \rightarrow P$, even though not directly measured, must be comparable. Thus, the lack of a multicomponent energy transfer process when B_L and B_M are excited together and the overall similarity of the energy transfer rates when initiated on the L and M sides lead to a consistent picture. If we argue further that energy transfer from $^1B_L \rightarrow P$ or $^1B_M \rightarrow P$ at low temperature cannot be accounted for by a Förster dipole−dipole mechanism, we are led to conclude that the matrix element governing energy transfer by an exchange mechanism appears to be comparable on the L and M sides for this step. On the other hand, energy transfer from ^1H_L (or $^1\beta_L$) $\rightarrow B_L$ or $^1H_M \rightarrow B_M$ may be occurring by a Förster dipole−dipole mechanism. Examination of the low-temperature absorption spectrum of the beta mutant (Figure 2B) indicates that the overlap between the hypothetical emission from $^1\beta_L$ with B_L should be greater than that of ^1H_M with B_M. A quantitative analysis depends on precise values for the Stokes shifts for $^1\beta_L$ and ^1H_M, which are not available, and an accurate deconvolution of the spectral line shapes of B_L and B_M, which is likewise not in hand. Nonetheless, we can qualitatively justify the somewhat faster rate of energy transfer from $^1\beta_L \rightarrow B_L$ than $^1H_M \rightarrow B_M$ (assuming the two-step sequential mechanism with the first step dominated by dipole−dipole interactions). A more detailed analysis would be very desirable, as it may be that this first energy transfer step also has a signficant contribution from an exchange mechanism, in which case we would conclude that the matrix elements for these steps are also comparable. This may be possible with other modified RCs.

The relative contributions of electronic coupling and free energy/reorganization energy to the observed unidirectional electron transfer starting from ^1P have been widely discussed. Because it has not been possible to measure the free energy of states such as $P^+B_M^-$ or $P^+H_M^-$ or the rates and temperature dependence of their formation, we have little experimental information on these key intermediates. Experiments that probe the electrostatic screening of the $P^+Q_A^-$ state by comparing the observed electrochromic bandshifts with those calculated in vacuum given the known charge distribution in $P^+Q_A^-$ and the sensitivity of the monomer absorption bands to external electric fields suggest that the average dielectric screening on the functional L side is greater than on the nonfunctional M side.[3] This could stabilize charge-separated intermediates on the functional side to a greater extent than on the nonfunctional side. This relative positioning of energies of charge-separated intermediates also emerges from electrostatic calculations,[5,6,51] though specific origins of the differences have not been identified, and there are large disagreements on the calculated absolute energies of charge-separated states. Even the mechanism of the forward electron transfer on the functional side is not established, the two dominant views being a two-step hopping mechanism, $^1P \rightarrow P^+B_L^- \rightarrow P^+H_L^-$, and a single-step mechanism, $^1P \rightarrow P^+H_L^-$, where $P^+B_L^-$ serves as a virtual intermediate enhancing the coupling between the initial and final states.

The singlet energy transfer results presented here bear on the question of the origin of unidirectional electron transfer,[52] but not on the mechanism of electron transfer along the functional branch of redox-active chromophores. Singlet energy transfer occurs with little change in the charge distribution of the molecules involved compared with that associated with electron transfer. The very weak temperature dependence of energy transfer is also consistent with this. We have argued above that the $^1B_L \rightarrow P$ and $^1B_M \rightarrow P$ energy transfer rates are comparable and that the mechanism, at least at low temperature, is dominated by electron exchange. Because the absorption spectra of B_L and B_M are quite similar, the electronic coupling between the $^1B_L \leftarrow B_L$ or $^1B_M \leftarrow B_M$ transitions and the $^1P \leftarrow P$ transition appears to be comparable. ^1B_L or ^1B_M are not identical to B_L^- or B_M^-, respectively; however, the involved orbitals are closely related. Thus, we can take the similarity of the $^1B_L \rightarrow P$ and $^1B_M \rightarrow P$ energy transfer rates as an indication that the orbital overlaps between P and B on the functional and nonfunctional sides are comparable. This leads to the suggestion that the dominant source of functional asymmetry in the RC resides in the interactions between the chromophores and their surroundings, which affect their redox potentials and the reorganization energy, rather than their interactions with each other, which affect primarily the electronic coupling.

Acknowledgment. This paper celebrates Robin Hochstrasser's many contributions to spectroscopy, especially in condensed phase and biological systems, that have inspired two generations of investigators. We thank N. Cherepy for discussions of vibronic structure in the RC. This work was supported in part by grants from the NSF Biophysics Program and the Stanford FEL Center, supported by the Office of Naval Research under Contract N00014-91-C-0170. Partial support from the NIH for acquisition of key components of the Ti:sapphire laser is also gratefully acknowledged.

References and Notes

(1) Deisenhofer, J.; Epp, O.; Sinning, I.; Michel, H. *J. Mol. Biol.* **1995**, *246*, 429−457.

(2) McDowell, L. M.; Gaul, D.; Kirmaier, C.; Holten, D.; Schenck, C. C. *Biochemistry* **1991**, *30*, 8315−8322.

(3) Steffen, M. A.; Lao, K.; Boxer, S. G. *Science* **1994**, *264*, 810−816.

(4) Plato, M.; Moebius, K.; Michel-Beyerle, M. E.; Bixon, M.; Jortner, J. *J. Am. Chem. Soc.* **1988**, *110*, 7279−7285.

(5) Marchi, M.; Gehlen, J. N.; Chandler, D.; Newton, M. *J. Am. Chem. Soc.* **1993**, *115*, 4178−4190.

(6) Parson, W. W.; Chu, Z.-T.; Warshel, A. *Biochim. Biophys. Acta* **1990**, *1017*, 251−272.

(7) Heller, B. A.; Holten, D.; Kirmaier, C. *Science* **1995**, *269*, 940−945.

(8) Jean, J. M.; Chan, C.-K.; Fleming, G. R. *Isr. J. Chem.* **1988**, *28*, 169−176.

(9) Scholes, G. D.; Ghiggino, K. P. *J. Phys. Chem.* **1994**, *98*, 4580−4590.

(10) Oevering, H.; Verhoeven, J. W.; Paddon-Row, M. N.; Cotsaris, E.; Hush, N. S. *Chem. Phys. Lett.* **1988**, *143*, 488−95.

(11) Closs, G. L.; Piotrowiak, P.; MacInnes, J. M.; Fleming, G. R. *J. Amer. Chem. Soc.* **1988**, *110*, 2652−2653.

(12) Franzen, S.; Goldstein, R. F.; Boxer, S. G. *J. Phys. Chem.* **1993**, *97*, 3040−3053.

(13) Förster, J. T. *Z. Naturforsch.* **1949**, *4a*, 321.

(14) Dexter, D. L. *J. Chem. Phys.* **1952**, *21*, 836−850.

(15) Craig, D. P.; Thirunamachandran, T. *Acc. Chem. Res.* **1986**, *19*, 10−16.

(16) Andrews, D. L.; Allcock, P. *Chem. Soc. Rev.* **1995**, *24*, 259−265.

(17) Scholes, G. D.; Clayton, A. H. A.; Ghiggino, K. P. *J. Chem. Phys.* **1992**, *97*, 7405−13.

(18) Breton, J.; Martin, J.-L.; Migus, A.; Antonetti, A.; Orszag, A. *Proc. Natl. Acad. Sci. U.S.A.* **1986**, *83*, 5121−5125.
(19) Breton, J.; Martin, J.-L.; Fleming, G. R.; Lambry, J.-C. *Biochemistry* **1988**, *27*, 8276−8284.
(20) Jia, Y.; Jonas, D. M.; Joo, T.; Nagasawa, Y.; Lang, M. J.; Fleming, G. R. *J. Phys. Chem.* **1995**, *99*, 6263−6266.
(21) Schenck, C. C.; Gaul, D.; Steffen, M.; Boxer, S. G.; McDowell, L.; Kirmaier, C.; Holten, D. In *Reaction Centers of Photosynthetic Bacteria*; Michel-Beyerle, M. E., Ed.; Springer-Verlag: Berlin, Heidelberg, 1990; Vol. 6, pp 229−238.
(22) Kirmaier, C.; Gaul, D.; Debey, R.; Holten, D.; Schenck, C. C. *Science* **1991**, *251*, 922−926.
(23) King, B. A.; Stanley, R. J.; Boxer, S. G. In preparation.
(24) Stanley, R. J.; Boxer, S. G. *J. Phys. Chem.* **1995**, *99*, 859−863.
(25) Goldsmith, J. G. Ph.D. Thesis, Stanford University, 1996.
(26) Goldsmith, J. G.; Boxer, S. G. *Biophys. J. Abstr.* **1995**, *68*, A325.
(27) Okamura, M. Y.; Isaacson, R. A.; Feher, G. *Proc. Natl. Acad. Sci. U.S.A.* **1975**, *72*, 3491−3495.
(28) Du, M.; Rosenthal, S. J.; Xie, X.; DiMagno, T. J.; Schmidt, M.; Hanson, D. K.; Schiffer, M.; Norris, J. R.; Fleming, G. R. *Proc. Natl. Acad. Sci. U.S.A.* **1992**, *89*, 8517−8521.
(29) Hamm, P.; Gray, K. A.; Oesterhelt, D.; Feick, R.; Scheer, H.; Zinth, W. *Biochim. Biophys. Acta* **1993**, *1142*, 99−105.
(30) Johnson, A. E.; Myers, A. B. *J. Chem. Phys.* **1996**, *104*, 2497−2507.
(31) Tang, J.; Norris, J., R. *Nucl. Inst. Methods Phys. Res.* **1988**, *A273*, 338−342.
(32) Wise, F. W.; Rosker, M. J.; Millhauser, G. L.; Tang, C. L. *IEEE J. Quantum Elec.* **1987**, *QE-23*, 1116−1121.
(33) Barkhuijsen, H.; De Beer, R.; Bovee, W. M. M. J.; Ormondt, D. v. *J. Magn. Reson.* **1985**, *61*, 465−481.
(34) Vos, M. H.; Rappaport, F.; Lambry, J.-C.; Breton, J.; Martin, J.-L. *Nature* **1993**, *363*, 320−325.
(35) Vos, M. H.; Jones, M. R.; Hunter, C. N.; Breton, J.; Lambry, J.-C.; Martin, J.-L. *Biochemistry* **1994**, *33*, 6750−6757.
(36) Vermeglio, A.; Clayton, R. K. *Biochim. Biophys. Acta.* **1976**, *449*, 500−515.
(37) Breton, J. *Biochim. Biophy. Acta* **1985**, *810*, 235−245.
(38) Xie, X.; Simon, J. D. *Biochim. Biophys. Acta* **1991**, *1057*, 131−139.
(39) Knapp, E. W.; Fischer, S. F.; Zinth, W.; Sander, M.; Kaiser, W.; Deisenhofer, J.; Michel, H. *Proc. Natl. Acad. Sci. U.S.A.* **1985**, *82*, 8463−8467.
(40) Ebrey, T. G.; Clayton, R. K. *Photochem. Photobiol.* **1969**, *10*, 109−117.
(41) Savikhin, S.; Struve, W. S. *Biophys. J.* **1994**, *67*, 2002−2007.
(42) Hamm, P.; Zinth, W. In *Ultrafast Phenomena VIII*; Martin, J.-L., Ed.; Springer-Verlag: Berlin, 1993; pp 541−542.
(43) Boxer, S. G.; Kuki, A.; Wright, K. A.; Katz, B. A.; Xuong, N. G. *Proc. Natl. Acad. Sci. U.S.A.* **1982**, *79*, 1121−1125.
(44) Haran, G.; Wynne, K.; Moser, C. C.; Dutton, P. L.; Hochstrasser, R. M. *J. Phys. Chem.* **1996**, *100*, 5562−5569.
(45) Wynne, K.; Haran, G.; Reid, G. D.; Moser, C. C.; Dutton, P. L.; Hochstrasser, R. M. *J. Phys. Chem.* **1996**, *100*, 5140−5148.
(46) Moog, R. S.; Kuki, A.; Fayer, M. D.; Boxer, S. G. *Biochemistry* **1984**, *23*, 1564−1571.
(47) Ermler, U.; Fritzsch, G.; Buchanan, S. K.; Michel, H. *Structure* **1994**, *2*, 925−936.
(48) We note that, contrary to the assertion of Haran et al.,[44] the directions of the transition dipole moments on the monomeric bacteriochlorophylls and the special pair in the RC are not accurately known in the molecular axis system. Although there is extensive dichroism data, such as the steady state fluorescence (Ebrey, T. G.; Clayton, R. K. *Photochem. Photobiol.* **1969**, *10*, 109−117), photobleaching of P870 (Vermeglio, A.; Clayton, R. K. *Biochim. Biophys. Acta.* **1976**, *449*, 500−515) and on stretched films (Breton, J. *Biochim. Biophys. Acta* **1985**, *810*, 235−245), which provide important information on the *projections* of these moments on each other or on the C_2 local symmetry axis, respectively, these are not absolute measurements of the directions of the moments.
(49) Scherer, P. O. J.; Fischer, S. F. *The Chlorophylls*; CRC Press: Boca Raton, FL, 1991; p 1079.
(50) We note that ^{1}H to P energy transfer could involve ^{1}B as a virtual intermediate rather than as a real intermediate; that is, energy transfer could be occurring by a superexchange mechanism. Some indirect evidence for this can be found in the interesting work of Hartwich et al. (Hartwich, G.; Friese, M.; Scheer, H.; Ogrodnik, A.; Michel-Beyerle, M. E. *Chem. Phys.* **1995**, *197*, pp 423−434), although these authors did not suggest this interpretation. These authors examined RCs in which the bacteriochlorophyll monomers were replaced with Ni-containing bacteriochlorophyll. The latter has a very rapid, nonradiative pathway to the ground state, and in contrast with native RCs, the steady state fluorescence excitation spectrum of ^{1}P in these modified RCs exhibits a dip at the B bands relative to the absorption spectrum. Interestingly, this dip is *not* observed for the H bands. If energy transfer in these RCs is occurring as ^{1}H to Ni−bacteriochlorophyll to P, then the excitation, once on the Ni−bacteriochlorophyll, should be lost to the same degree as it would be upon direct excitation, and the H bands should also be depressed in the fluorescence excitation spectrum. As this is apparently not the case, it suggests that the singlet excited state of Ni−bacteriochlorophyll may not actually be formed during ^{1}H to P energy transfer. Orbital overlap of the type required for superexchange via the excited state of Ni−bacteriohlorophyll would not be greatly affected by Ni-substitution, so this is a plausible mechanism.
(51) Gehlen, J. N.; Marchi, M.; Chandler, D. *Science* **1994**, *263*, 499−501.
(52) We note that triplet energy transfer ^{3}P → B_M → carotenoid must be dominated by an exchange mechanism, as the electronic transitions are forbidden. Measurements of the ^{3}P energy (Takiff, L.; Boxer, S. G. *Biochim. Biophys. Acta* **1988**, *932*, 325−334) and that of the triplet state of monomeric bacteriochlorophyll in solution (Takiff, L.; Boxer, S. G. *J. Am. Chem. Soc.* **1988**, *110*, 4425−4426) place the triplet state of monomer B chromophores somewhat above that of ^{3}P, making allowances for the shift of the B absorption from that of an isolated bacteriochlorophyll in solution. The energy gap is consistent with the observed activation energy for ^{3}P → carotenoid energy transfer. Because there is no carotenoid near B_L, it is unfortunately not possible to measure the asymmetry in electronic coupling using triplet energy transfer.

JP9614916